ORIGINAL RESEARCH PAPER
Volume - 13 | Issue - 11 | November - 2024 | PRINT ISSN No. 2277 - 8179 | DOI : 10.36106/ijsr
INTERNATIONAL JOURNAL OF SCIENTIFIC RESEARCH

UNCERTAINTY QUANTIFICATION FOR DEEP LEARNT ANOMALOUS GEOMAGNETIC STORM FORECASTING

Computer Science

Yashasvika Ahuja Student, Department of Computer Science ALLEN career institute "SANKLAP",CP-6, Indra Vihar ,KOTA ,RAJASTHAN 324005.

Ashish Kumar Sharma Professor Department of Computer Science, ALLEN career institute "SANKLAP",CP-6, Indra Vihar, KOTA, RAJASTHAN 324005.

ABSTRACT

We present a multitask transformer-based network that forecasts geomagnetic storms by incorporating phys- ical laws into the proposed model. By restricting the search space, our model predicts the Sym − H, Ap, and Kp indices, commonly used as proxies geomagnetic activities. We aim to improve upon previous models that rely solely on solar-wind indices. With ample data available since 1930s, our model is trained on high-resolution data set for accurate and reliable forecasts of one of the most severe geomagnetic storms. The impact of geomagnetic storms on electric grids and communication systems necessitates accurate forecasts with uncertainty bounds, which is the primary objective of our work presented in this paper.

KEYWORDS

Geomagnetic Storm, Deep Learning, Space Weather

INTRODUCTION

Geomagnetic storms represent one of the most se vere space-weather phenomena, with extensive im pacts on space-borne satellite systems, terrestrial electric grids, and communication systems Geomagnetic storms arise from rapid, transient fluctuations in the earth's magnetic field caused by the magnetic field, density, velocity of the solar wind and and the degree of its impact is governed by complex physical laws The complex nature of the coupling of magnetosphere-ionosphere system pose a formidable challenge in developing accurate models to forecast their occurrence. These impacts have motivated ex- tensive research to understand the link among solar processes, interplanetary phenomena, and resulting geomagnetic activity and to forecast the occurrence of such activities.

The prediction of geomagnetic storms has a long history. Researchers have employed analytical equations (Akasofu (1981), O'Brien & McPherron (2000), Boynton et al. (2011), Nikolaeva et al. (2011)), and statistical methods (Caswell (2014), Riley & Love (2017), Pulkkinen et al. (2011) and reference therein) to analyze and forecast these events. The majority of the previous studies have concentrated on predicting the Kp index, which serves as a prevalent measure of geomagnetic activity (Chakraborty & Morley (2020); Tan et al. (2018); Domico et al. (2022)) on a plan etary level. This index is calculated based on the range of deviation of the most disturbed horizontal component of the magnetic field from a quiet day in a hour interval (Kauristie et al. (2017)). In addition to the Kp index, the Dst (disturbance storm time) index is also used to identify and evaluate the strength and phases of a geomagnetic storm. The Dst index primarily reflects the ring current created by the gradient and curvature drifts of charged parti cles in the earth's magnetic field in addition to gyro and bounce motions and is calculated as the average hourly deviation of the H component of the magnetic field measured by several stations around the earth. Sym −H index represents the symmetric part of the 43 ring current and provides the strength of the ring current at higher temporal resolution (1 min as com pared to 1 hour resolution of Dst index). Thereforethis is practically the high cadence Dst index. The disadvantage of using statistical methods for predicting geomagnetic storms is that these models may not capture the complex, nonlinear relationships between the input variables and the output parameter due to the influence of a large number of factors such as so lar wind speed, Interplanetary Magnetic Field (IMF) strength, and the orientation of the IMF with respect to the Earth's magnetic field. This also highlights the need for more advanced models that can better represent the data and provide more reliable forecasting for these events.

In recent years, the research community has turned to machine learning techniques, particularly neural networks, to predict geomagnetic storms, owing to the availability of large data sets and the advances in this field (Wu & Lundstedt (1996), Wu & Lund stedt (1997), Siddique & Mahmud (2022), Tasistro Hart et al. (2021); Cristoforetti et al. (2022); Sid dique & Mahmud (2022)). High resolution data for many observational parameters related to the geo-magnetic activity is now publicly available, making complex neural networks a promising alternative to physical models. Cristoforetti et al. (2022) imple mented Long Short Term Memory (LSTM) based method for geomagnetic storm prediction. Siddique & Mahmud (2022) used an ensemble of multiple deep-learning-based models (such as Recurrent Neural Networks (RNNs) and LSTM Networks) for predicting the ground magnetic perturbations.

They also performed uncertainty quantification of these deep learning models using the Gaussian process and Bayesian Inference. The performance of these works underscores the potential of deep learning based methods in this domain.

It is worthwhile to state at this juncture that the accurate forecasting of geomagnetic storms by machine learning models is not always guaranteed. To ensure the reliability of predictions, it is important not only to determine the predicted value but also to quantify the probability or uncertainty associated with the prediction. Researchers in this field have recognized the significance of uncertainty quantifica tion. Tasistro-Hart et al. (2021) proposed an LSTM based architecture that produces forecasts and returns an uncertainty-based score (using the Gaus sian Process regression method) that indicates the probability of the occurrence of a given event. Simi larly, Chakraborty & Morley (2020) developed a deep learning model based on LSTM for forecasting the Kp index that incorporates a probabilistic framework (Gaussian process regression) to quantify uncertainty in geomagnetic storm predictions. These studies highlight the importance of incorporating uncertainty quantification in machine learning-based methods for predicting geomagnetic storms reliably.

Although previous approaches have yielded usefulresults in predicting geomagnetic storms, there re mains significant room for improvement. A key limi tation is the lack of exploration into the relationship between inferred patterns and the underlying phyical systems that generate these events.Moreover, traditional techniques have not been able to effec tively forecast the occurrence of the most severe and destructive geomagnetic storms, which are rare and typically happen only once per decade (Cristofore tti et al. (2022)). Given the potentially devastat ing consequences of such storms on modern techno logical systems, their accurate prediction and timely warning are of paramount importance. To overcome these challenges, novel approaches are required that can enhance the accuracy and reliability of geomagnetic storm forecasting. A promising direction is to leverage deep machine learning architectures that can effectively capture intricate temporal relation ships within time series datasets. In contrast, tradi tional shallow architectures are limited in this regard and may only achieve mid-range anomaly detection (Cristoforetti et al. (2022) Previous research has been limited by its narrow focus on predicting only the Kp and Dst indices in dependently, without exploiting the unique physical characteristics that different indices represent. To address this limitation, we have developed a multitask

learning framework that utilizes all available indices, including Sym H, Ap, and Kp, to enhance the accuracy of our model. Specifically, we have incor porated the Sym-H index, which provides a higher resolution version of the Dst index, into our frame work. With continuous data available for these in dices dating back to the 1930s for Kp, 1950s for Dst, laws, we effectively constrain the search space and enhance the reliability of our forecasts for the Sym- H, Kp, and Ap indices. Unlike shallow architectures, our deep learning model is capable of capturing in tricate relationships in time-series data and produc- ing highly accurate predictions. To further improve the reliability of our model, we have implemented an uncertainty-based score that estimates the probability of a given event. Overall, our approach represents a significant advance in the field of geomagnetic storm forecasting and holds great promise for improving our ability to predict these potentially destructive events.

MACHINE LEARNING MODELS FOR FORECASTING

In this section, we describe five machine learning and deep learning methodologies and their usage in our case.

ARTIFICIAL NEURAL NETWORKS

Artificial neural networks (ANNs) are a widely used method for approximating complex nonlinear functions through a series of elementary nonlinear functions. A trained ANN contains an implicit non- linear relationship between inputs and outputs and can be used for ionosphere prediction using only in- put features. The output of the network, given an input vector X, can be expressed as a function of the weights w and bias b, and activation function as,

$$y = k\left(\sum_{j=1}^{n} w_j x_j + b\right)$$

inputs and outputs, and in this study, the Rectified Linear Unit (ReLU) is used as the activation function. The structure of the ANN used in TEC forecasting is illustrated in Figure 1. The backpropagation algo rithm is employed to train the ANN model (Rojas & Rojas (1996).

LSTM NEURAL NETWORKS

Long Short Term Memory (LSTM) is a type of Recurrent Neural Network (RNN) that is well-suited for processing sequential data (H In a LSTM, information is stored in memory cells, and the network can selectively remember or forget information based on the input and previous state.

The forget gate controls the amount of previously stored information that is discarded from the memory cell. The input gate controls the portion of new in formation that is incorporated into the memory cell. The candidate cell state represents the newly pro posed memory value. The output gate regulates the extent to which the memory cell value is output. The activation function tanh is used to compress the val ues within the range of 1 to 1. This range restriction aids in stabilizing the gradients during the training process.

GRADIENT-BOOSTED DECISION TREES

Gradient Boosted Decision Trees (GBDT) build a set of decision trees and combines them to make 203 predictions. The goal is to minimize the loss func tion, which measures the difference between the predicted value and the true value. The GBDT algo rithm works by iteratively training decision trees to correct the residual errors made by the previous tree (Dorogush et al. (2018) Al Daoud (2019)).

At each iteration, a new decision tree is trained to predict the negative gradient of the loss function with respect to the current model's output. The output of the model at each iteration is the sum of the pre where j ranges from 1 to n. The activation function introduces non-linearity to the relationship between dictions from all previously trained trees, multiplied by a learning rate that controls the contribution of each tree. This can be expressed mathem atically as data and extracts features that are relevant for the follows:Chen et al. (2015) downstream prediction task. The encoder consists of a stack of identical layers, each of which has two sub

$$F_m(x) = F_{m-1}(x) + \gamma \cdot h_m(x)$$

where Fm(x) is the model prediction at round m,

layers: a multi-head self-attention mechanism and aposition wise feed-forward network (Li et al. (2019)).

The self-attention mechanism in the encoder allows

$F_{m-1}(x)$ is the model prediction at round m ¯ 1, hm(x) is the weak learner at round m, and γ is the learning rate which controls the contribution of each tree. The loss function is defined as: each position in the input sequence to attend to all other positions and capture their interactions. This helps the model to capture long-range dependencies in the time series data, which can be crucial for ac- curate predictions. The feed-forward network in the encoder then applies a non-linear transformation to the output of the self-attention mechanism to further 260 refine the feature representation.

$$L(F_m(x), y) = \sum_{i=1} l(F_{m-1}(x_i) + \gamma \cdot h_m(x_i), y_i)$$

where y_i is the true label of the i-th example, l isby the encoder, the resulting feature representation is the loss function, and n is the number of examples.passed on to the decoder, which generates the output The weak learner $h_m(x)$ is a decision tree thattime series sequence. Like the encoder, the decoder is trained to minimize the negative gradient of thealso consists of a stack of identical layers, each of loss function with respect to the model prediction atwhich has two sub-layers: a multi-head self-attention round m ¯ 1:mechanism and a multi-head attention mechanism over the encoder outputs.

$$h_m(x) = \arg\min_h \sum_{i=1}^{n} \frac{\partial L(F_{m-1}(x), y)}{\partial F_{m-1}(x_i)} - h(x_i)$$

The self-attention mechanism in the decoder allows each position in the output sequence to attend to each position in the output sequence to attend to helps to capture the temporal dependencies between where arg min denotes the function that minimizes the output values. The multi-head attention mech the expression within the brackets.anism over the encoder outputs allows the decoder to attend to different parts of the input sequence

ATTENTION-BASEDTRANSFORMERS

The transformer architecture has become increas- ingly popular in the field of natural language process- ing, with its ability to capture longrange dependen depending on the current position in the output se quence. Finally, a position-wise feed-forward network in the decoder is used to transform the output of the self-attention and multi-head attention mechanisms 280 into the final predicted values.

A rough algorithm for the basic transformer archi cies and model complex interactions between tokens in a sequence. The transformer is based on an atten- tion mechanism that allows each token to attend to all other tokens in the sequence, enabling the model to capture both local and global dependencies. This tecture can be described as follows (Vaswani et al. (2017)). has led to significant improvements in tasks such as machine translation and text generation, as well as time series analysis (Vaswani et al. (2017)).

EXPERIMENTAL SETUP

In the encoder-decoder architecture of a trans The dataset has been curated considering the faformer for time series analysis, the input time series tors that affect alterations in geomagnetic storms and data is first fed into an encoder, which processes the activities.

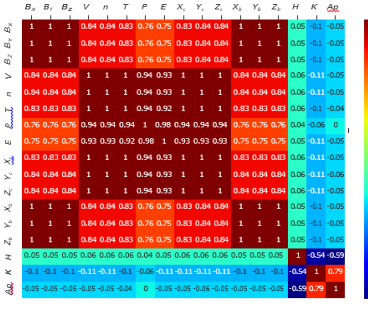

Figure 1:

DATASET FEATURE SELECTION

The parameters have been selected based on the feature importance score obtained by using the Ran- dom forest method. Random Forest calculates the feature importance score using a technique called Gini impurity or Mean Decrease in Impurity (MDI). During the

construction of each decision tree in the forest, the algorithm repeatedly splits the data based on features, selecting the feature that results in the greatest reduction in impurity (measured by the Gini impurity or entropy). The feature importance score is then calculated by summing up the reduction in impurity caused by each feature across all the decision trees in the forest. Features with a higher total reduction in impurity are considered more important as they contribute more to the predictive accuracy of the Random Forest model. The final set of features is listed in table

Table 1: 2-Letter Representative Names, Definitions, and Fea- ture importance, with the selected features in bold.

Names	Definition	F_{imp}
Bx	**Magnetic field component in X direction (GSE)**	0.85
By	**Magnetic field component in Y direction (GSE)**	0.90
Bz	**Magnetic field component in Z direction (GSE)**	0.88
V x	**Solar wind flow speed in X direction (GSE)**	0.87
V y	**Solar wind flow speed in Y direction (GSE)**	0.92
V z	**Solar wind flow speed in Z direction (GSE)**	0.86
E	**Electric field strength (mV/m)**	0.95
n	**Proton density (n/cc)**	0.94
T	**Temperature (K)**	0.93
P	**Solar wind flow pressure (nPa)**	0.91
Xc	Spacecraft position component in X direction (GSE)	0.23
Y c	Spacecraft position component in Y direction (GSE)	0.06
Zc	Spacecraft position component in Z direction (GSE)	0.05
Xb	BSN position component in X direction (GSE)	0.09
Y b	BSN position component in Y direction (GSE)	0.07
Zb	BSN position component in Z direction (GSE)	0.09
H	Sym/H index (nT)	0.06
K	3-hourly KP index (scaled by 10)	0.05
Ap	3-hourly Ap index (nT)	0.06

Table 2: Table showing the input parameters and the refer- enced indexes.

Inputs	Outputs
Interplanetary Magnetic field (B_x, B_y, B_z) Magnetic flow Velocity (V_x, V_y, V_z) Electric Field Magnitude (E) Proton Density Temperature Flow Pressure	*Sym*-H Index K_P Index A_P Index

Criteria	Definition	Equation
RMSE	Root mean square value	$\sqrt{\frac{1}{N}\sum_{i=1}^{N}(y_i - \hat{y}_i)^2}$
MAE	Mean absolute error	$\frac{1}{N}\sum_{i=1}^{N}\lvert y_i - \hat{y}_i\rvert$
MAPE	Mean Abs. Pct. error	$\frac{1}{N}\sum_{i=1}^{N}\frac{\lvert y_i - \hat{y}_i\rvert}{\lvert y_i\rvert} \times 100\%$
R^2	Coeff. of determination	$1 - \frac{\sum_{i=1}^{N}(y_i - \hat{y}_i)^2}{\sum_{i=1}^{N}(y_i - \bar{y})^2}$

DATASET ANALYSIS

The dataset consists of parameters that corre- spond to the interplanetary magnetic field, solar wind plasma, and various geomagnetic indices. The data was collected from NASA's CDAWeb portal. In ad- dition to the magnetic field parameters, we have in- cluded other relevant variables such as magnetic flow velocity (Vx, Vy, Vz), electric field magnitude, pro- ton density, temperature, and flow pressure. We are using three indices to measure geomagnetic activity: Sym-H, AP Index, and KP Index. These 318 indices provide measures of the perturbation in the 319 Earth's magnetic field caused by solar wind and other 320 space weather phenomena.

The SYM-H index measures the maximum pertur bation of the horizontal component of the Earth's magnetic field and is derived from magnetometer data collected at low-latitude observatories. The AP index is a planetary index of geomagnetic activity derived from the Kp index, calculated from

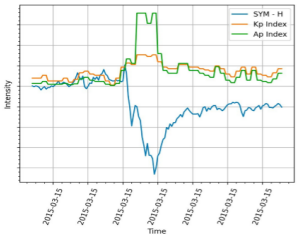

Figure 2: Variation in various indices during the St. Patrick's Day storm.

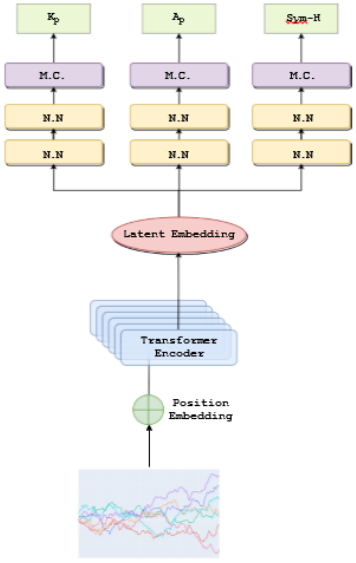

Figure 3:

measurements at 13 sub-auroral observatories. The Kp index categorizes geomagnetic activity in quasi- logarithmic steps ranging from 0 to 9, where a higher number indicates a higher level of geomagnetic dis- turbance. We followed the convention developed by to indicate that a Kp index value of 0- 1 corresponds to a quiet range, while a value greater than 4 indicates a disturbed range. The AP index is a linearly mapped index that measures the disturbance 20 train-validation split. The testing data is from 8th August 2017 - 31st December 2021. The time period in the magnetic field on a planetary scale. for train and test is ideal since it innately covers dorWe hypothesize that using three different indices, m a n t p e r i o d s accompanied by major solar storms, for SYM-H, AP, and KP, as labels for our transformer example, the solar storms of November 2003. Our 340 based approach for geomagnetic space weather pre- test dataset covers the Saint Patrick's Day storm, diction time series task will allow us to capture the which will be crucial in analyzing the performance of nuances of the geomagnetic activity and provide a our model. more comprehensive understanding of space weather Time series analysis is a statistical technique used conditions. Furthermore, previous research has prito predict future geomagnetic behavior by analyzing marily focused on using single indices, such as the Dst data for patterns and trends. or SYM-H index, on predicting geomagnetic storms.

METHODOLOGY AND PIPELINE

By using three different indices, we introduce nov elty and potential improvements to existing prediction models. The training data is 1st January 2000 - 7th August 2017. This dataset will further be divided into a 80 The training data is 1st January 2000 - 7th AugustMultitask learning of the Sym − H, Ap, and Kp364351 2017. This dataset will further be divided into a 80-indices can be used to improve the accuracy of predictions for solar storms. Each of these indices pro- vides information on different aspects of the Earth's magnetic field, and by combining them in a multitask learning approach, we can leverage the complemen- tary information they provide to make more accurate predictions.

The Sym − H index measures the overall strength of the Earth's magnetic field, the AP index measures the strength of the magnetic disturbances in the iono- sphere, and the KP index measures the strength of magnetic disturbances caused by solar winds. To- gether, these indices provide a more comprehensive view of the state of the Earth's magnetic field and can be used to predict the likelihood of a solar storm.

Table 3: The prediction scores on Kp in related work. The metrics are as reported in and

Algorithm	RMSE (3 hour)
RNN	0.93
XGBoost	1.24

Random Forest (Seq-2-Seq)	0.57
Ours(without multitask)	0.51
Ours(with multitask)	0.48

Table 4: The prediction scores on DsT in related work. The metrics are as reported in

Algorithm	RMSE (3 hour)
BRANN	3.784
LR Stepwise	9.569
LSTM	12.21
Ours(without multitask)	3.23
Ours(with multitask)	3.01

Table 5: The prediction scores on SYM-H in related work. The metrics are as reported in

Algorithm	RMSE 3 hour
GBM (Gradient Boosting Machine)	7.412
LSTM 1 (Siciliano et al., 2021)	7.860
LSTM 2 (Collado-Villaverde et al., 2021)	8.550
Ours(without multitask)	7.056
Ours(with multitask)	6.798

RESULTS AND DISCUSSION

We employed a transformer-based multitasking ar- chitecture to forecast three important space weather parameters, namely Kp, Sym − H, and Ap values. We compared our proposed model with state-of-the-art architectures and various machine learning meth- ods. Our experiments involved training the model on a large historical space weather data dataset and evaluating its performance using rigorous eval- uation metrics. We also conducted ablation studies to investigate the impact of different components of our proposed architecture. The experimental results demonstrate the effectiveness and superiority of our We employed a transformer-based multitasking ar- chitecture to forecast three important space weather parameters, namely Kp, Sym − H, and Ap values. We compared our proposed model with state-of-the-art architectures and various machine learning meth- ods. Our experiments involved training the model on a large historical space weather data dataset and evaluating its performance using rigorous eval- uation metrics. We also conducted ablation studies to investigate the impact of different components of our proposed architecture. The experimental results demonstrate the effectiveness and superiority of our AlgorithmRMSE 3 hourGBM (Gradient Boosting Machine)7.412LSTM 1 (Siciliano et al., 2021)7.860LSTM 2 (Collado-Villaverde et al., 2021)8.550Ours(without multitask)7.056Ours(with multitask)6.798Table 5: The prediction scores on SYM-H in related work. The metrics are as reported in A key aspect of our predictions is the uncertainty 409 bound that accompanies the predicted value. Figure shows the prediction on the Kp index along with the uncertainty bound at every step of prediction. transformer-based multitasking architecture in accurately predicting Kp, Sym−H, and DsT values com-

CONCLUSION

pared to existing approaches, highlighting the poten-This study presents a transformer-based multitasktial of transformer-based models for space weathering architecture for forecasting three critical space415398 forecasting applications. The Sym H values haveweather indices, namely Kp, Sym H, and Ap. It been extrapolated to predict the DsT . This is perhighlights the potential of transformer-based mod-417400 the findings of whichels for accurate and reliable space weather forecast identifies Sym H as a de-facto high-resolution ver-ing applications. Our work contributes to the devel-419402 sion of DsT .opment of advanced forecasting techniques to miti-420403 As observed from T T and T re-gate the impact of space weather on various critical spectively, multitasking has performed better thansystems, including communication netw single-task methods. More importantly, multitasking and power grids(Radasky reduces the uncertainty in the prediction of individual 424407 indices, thus allowing for more robust and accurateThe proposed architecture provides state-of-the-art predictions.results in geomagnetic indices such as K_p, Sym H, and DsT predictions. In addition to its superior per- formance, our transformer-based multitasking archi- tecture provides uncertainty bounds along with its predictions, as can be seen in This feature is crucial for decision-making in critical applications such as space weather forecasting, where the conse- quences of false alarms or missed alerts can be ex-treme. Further research can explore approaches to im- prove the estimation of uncertainty bounds and their incorporation into decision-making processes for space weather applications. The integration of other data sources and physical models to further improve the accuracy and generalization capability of transformer-based models for space weather forecast- ing provide vast scope for future work in this domain.

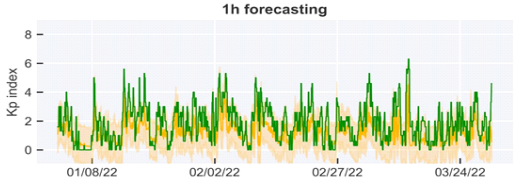

Figure 4: Prediction results on our architecture. Green is our ground truth, orange is the prediction, and the translucent region represents our uncertainty bound.

REFERENCES

1. Akasofu, S.-I. (1981). Prediction of development ofgeomagnetic storms using the solar wind- magnetosphere energy coupling function . Plan-etary and Space Science, 29 (11), 1151–1158.
2. Al Daoud, E. (2019). Comparison between xgboost, lightgbm and catboost using a home credit dataset. International Journal of Computer and Informa- tion Engineering , 13 (1), 6–10.
3. Bartels, J. (1963). Discussion of time-variations of ge- omagnetic activity, indices Kp and Ap, 1932-1961. Annales de Geophysique, 19 , 1.
4. Boteler, D., Pirjola, R., & Nevanlinna, H. (1998). The effects of geomagnetic disturbances on elec- 4 trical systems at the earth's surface. Advances in Space Research, 22 (1), 17–27.
5. Boynton, R., Balikhin, M., Billings, S. et al. (2011). Data derived narmax dst model. In Annales geo- physicae (pp. 965–971). Copernicus Publications G¨ottingen, Germany volume 29.
6. Caswell, J. M. (2014). A nonlinear autoregressive approach to statistical prediction of disturbance storm time geomagnetic fluctuations using solar data. Journal of Signal and Information Process- ing, 2014 .
7. Chakraborty, S., & Morley, S. K. (2020). Probabilis- tic prediction of geomagnetic storms and the kp index. Journal of Space Weather and Space Cli- mate, 10 , 36.
8. Chen, T., He, T., Benesty, M. et al. (2015). Xgboost: extreme gradient boosting. R package version 0.4- 2 , 1 (4), 1–4.
9. Cristoforetti, M., Battiston, R., Gobbi, A. et al. (2022). Prominence of the training data prepa- ration in geomagnetic storm prediction using deep neural networks. Scientific Reports, 12 (1), 7631.
10. Domico, K., Sheatsley, R., Beugin, Y. et al. (2022). A machine learning and computer vision approach to geomagnetic storm forecasting. arXiv preprint arXiv:2204.05780 , .
11. Dorogush, A. V., Ershov, V., & Gulin, A. (2018). Catboost: gradient boosting with categorical fea- tures support. arXiv preprint arXiv:1810.11363 ,
12. Gulati, I., Tiwari, R., Johnston, M. et al. (2019).
13. Nikolaeva, N., Yermolaev, Y., & Lodkina, I. (2011). Dependence of geomagnetic activity during mag- netic storms on the solar wind parameters for dif- ferent types of streams. Geomagnetism & Aeron- omy, 51 (1).
14. O'Brien, T. P., & McPherron, R. L. (2000). Forecast- ing the ring current index dst in real time. Jour- nal of Atmospheric and Solar-Terrestrial Physics, 62 (14), 1295–1299.
15. Pulkkinen, A., Kuznetsova, M., Ridley, A. et al. (2011). Geospace environment modeling 2008–2009 challenge: Ground magnetic field perturbations. Space weather , 9 (2). Radasky, W., & Kappenman, J. (2010).Im- pacts of geomagnetic storms on ehv and uhv power grids. 2010 Asia-Pacific Symposium on Electromagnetic Compatibility, APEMC 2010 , . 10.1109/APEMC.2010.5475523.
16. Impact of solar flares on hf radio communication at high latitude. In 2019 International Confer- ence on Automation, Computational and Tech- nology Management (ICACTM) (pp. 550–554). 10.1109/ICACTM.2019.8776851.
17. Hu¨sken, M., & Stagge, P. (2003). Recurrent neural networks for time series classification. Neurocom- puting , 50 , 223–235.
18. Iong, D., Chen, Y., Toth, G. et al. (2022). New find- ings from explainable SYM-h forecasting using gra- dient boosting machines, .
19. Jain, A. K., Mao, J., & Mohiuddin, K. M. (1996). Artificial neural networks: A tutorial. Computer , 29 (3), 31–44.
20. Kauristie, K., Morschhauser, A., Olsen, N. et al. (2017). On the usage of geomagnetic indices for data selection in internal field modelling. Space ScienceReviews, 206 , 61–90.
21. Li, S., Jin, X., Xuan, Y. et al. (2019). Enhancing the locality and breaking the memory bottleneck of transformer on time series forecasting. Advances in neural information processing systems, 32 .
22. Riley, P., & Love, J. J. (2017). Extreme geomagnetic storms: Probabilistic forecasts and their uncertain- ties. Space Weather , 15 (1), 53–64.
23. Rojas, R., & Rojas, R. (1996). The backpropagation algorithm. Neural networks: a systematic intro- duction, (pp. 149–182).
24. Sexton, Ernest Scott, Nykyri, Katariina, & Ma, Xu- anye (2019). Kp forecasting with a recurrent neural network. J. Space Weather Space Clim., 9 , A19. SHIN, S., Son, J., Yi, K. et al. (2020).
25. Forecast- ing Kp Index Using a Hybrid Machine Learning Model Based on Random Forest and Sequence-to sequence.In AGU Fall Meeting Abstracts (pp. NG004–0018). volume 2020.
26. Siami-Namini, S., Tavakoli, N., & Namin, A. S. 542 (2019). The performance of lstm and bilstm in fore- 543 casting time series. In 2019 IEEE International Conference on Big Data (Big Data) (pp. 3285– 3292). 10.1109/BigData47090.2019.9005997.
27. Siami-Namini, S., Tavakoli, N., & Siami Namin, (2018).A comparison of arima and lstm in forecasting time series.In 2018 17th IEEE International Conference on Machine Learn- ing and Applications (ICMLA) (pp. 1394–1401). 10.1109/ICMLA.2018.00227.
28. Siddique, T., & Mahmud, M. S. (2022).Ensem- ble deep learning models for prediction and uncer- tainty quantification of ground magnetic perturba- tion. Frontiers in Astronomy and Space Sciences, 9 , 1031407.
96. Tan, Y., Hu, Q., Wang, Z. et al. (2018). Geomagnetic index kp forecasting with lstm. Space Weather , 16 (4), 406–416.
99. Tasistro-Hart, A., Grayver, A., & Kuvshinov, A. (2021). Probabilistic geomagnetic storm forecast- ing via deep learning. Journal of Geophysical Re- search: Space Physics, 126 (1), e2020JA028228.
100. Vaswani, A., Shazeer, N., Parmar, N. et al. (2017).
101. Attention is all you need. Advances in neural in- formation processing systems, 30 .

102. Wang, J., Luo, B., Liu, S. et al. (2023). A machine learning-based model for the next 3 day geomag- netic index (kp) forecast. Frontiers in Astronomy and Space Sciences, 10 .
103. Wang, S., Dehghanian, P., Li, L. et al. (2019). A ma- chine learning approach to detection of geomagnet- ically induced currents in power grids. IEEE Trans- actions on Industry Applications, 56 (2), 1098– 1106.
104. Wanliss, J. A., & Showalter, K. M. (2006). High- resolution global storm index: Dst versus SYM-H.
105 Journal of Geophysical Research (Space Physics), 111 (A2), A02202. 10.1029/2005JA011034.
106. Wu, J.-G., & Lundstedt, H. (1996). Prediction of geomagnetic storms from solar wind data using el- man recurrent neural networks. Geophysical re- search letters, 23 (4), 319–322.
107. Wu, J.-G., & Lundstedt, H. (1997). Geomagnetic storm predictions from solar wind data with the use of dynamic neural networks. Journal of Geo- physical Research: Space Physics, 102 (A7), 14255– 14268.